Author Manuscript

Author Manuscript

Author Manuscript

Author Manuscript

HHS Public Access

Author manuscript

Brain Stimul. Author manuscript; available in PMC 2020 December 08.

Published in final edited form as:

Brain Stimul. 2020 ; 13(6): 1548–1558. doi:10.1016/j.brs.2020.08.017.

Entrainment of cerebellar purkinje cells with directional AC electric fields in anesthetized rats

Ahmet S. Asan[a], **Eric J. Lang**[b], **Mesut Sahin**[a,*]

[a]Department of Biomedical Engineering, New Jersey Institute of Technology, University Heights, Newark, NJ, 07102, USA

[b]Department of Neuroscience and Physiology, New York University School of Medicine, Science Building, New York, NY, 07102, USA

Abstract

Background—Transcranial electrical stimulation (tES) shows promise to treat neurological disorders. Knowledge of how the orthogonal components of the electric field (E-field) alter neuronal activity is required for strategic placement of transcranial electrodes. Yet, essentially no information exists on this relationship for mammalian cerebellum *in vivo*, despite the cerebellum being a target for clinical tES studies.

Objective—To characterize how cerebellar Purkinje cell (PC) activity varies with the intensity, frequency, and direction of applied AC and DC E-fields.

Methods—Extracellular recordings were obtained from vermis lobule 7 PCs in anesthetized rats. AC (2–100 Hz) or DC E-fields were generated in a range of intensities (0.75–30 mV/mm) in three orthogonal directions. Field-evoked PC simple spike activity was characterized in terms of firing rate modulation and phase-locking as a function of these parameters. t-tests were used for statistical comparisons.

Results—The effect of applied E-fields was direction and intensity dependent, with rostrocaudally directed fields causing stronger modulations than dorsoventral fields and mediolaterally directed ones causing little to no effect, on average. The directionality dependent modulation suggests that PC is the primary cell type affected the most by electric stimulation, and this effect was probably given rise by a large dendritic tree and a soma. AC stimulation entrained activity in a frequency dependent manner, with stronger phase-locking to the stimulus cycle at higher frequencies. DC fields produced a modulation consisting of strong transients at current onset and offset with an intervening plateau.

This is an open access article under the CC BY-NC-ND license (http://creativecommons.org/licenses/by-nc-nd/4.0/).

*Corresponding author, sahin@njit.edu (M. Sahin).

CRediT authorship contribution statement

Ahmet S. Asan: Data curation, Formal analysis, Visualization, Writing - original draft. **Eric J. Lang:** Funding acquisition, Methodology, Writing - review & editing. **Mesut Sahin:** Conceptualization, Funding acquisition, Project administration, Writing - review & editing.

Declarations of competing interest

None.

Author Manuscript Author Manuscript Author Manuscript Author Manuscript

Conclusion—(s): Orientation of the exogenous E-field critically determines the modulation depth of cerebellar cortical output. With properly oriented fields, PC simple spike activity can strongly be entrained by AC fields, overriding the spontaneous firing pattern.

Keywords

Electrical stimulation; Cerebellar modulation; Spike entrainment; Transcranial direct current stimulation (tDCS); Transcranial alternating current stimulation (tACS)

Introduction

Electrical neuromodulation methods may be used to treat a wide variety of neurological disorders [1]. One such method that is generating significant interest is low intensity transcranial electrical stimulation (tES) because it is non-invasive, safe, has minimal to no side effects, and has a low-cost [2,3]. This method involves passing current through a specific brain region, and has been reported to improve performance and learning in both healthy individuals and in those with brain injury [4,5]. Indeed, tES has been found to have beneficial effects when applied to a number of different brain areas, including specific regions of the cerebral and cerebellar cortices [6,7]. Although such positive reports highlight the potential of tES, other studies have shown no results or negative ones [8,9]. The causes of this variability need to be understood in order for tES to reach its potential.

The cerebellum is one area in which the need to understand how tES acts stands out. Cerebellar tES (ctES) has been used to ameliorate motor deficits [10,11], consistent with its central role in motor function. Moreover, a growing body of evidence indicates that the cerebellum plays important roles in cognitive functions as well [12,13], which implies that ctES could be used to treat a wider variety of disorders. Indeed, clinical studies have shown that ctES, using either direct and alternating current, tDCS and tACS, can enhance both motor and cognitive functions [11,14,15]. This makes understanding how tES acts on the cerebellum and how it affects its output significant, as such knowledge would allow ctES treatments to be optimized.

The cerebellar cortex is likely to be the main area that is directly affected by ctES, given its superficial location. ctES will affect multiple classes of cerebellar cortical cells; however, the Purkinje cell (PC) is the sole output of the cortex, making characterization of its responses a key issue. PCs generate simple and complex spikes, the former spontaneously and in response to granule cell inputs, and the latter driven by climbing fiber activity. The spatiotemporal pattern of simple and complex spikes is important because synchronous PC activity sculpts the output of the cerebellar nuclei (CN) [16–19], which, in turn originate most cerebellar output, including projections, via the thalamus, to widespread regions of the cerebral cortex (i.e., motor, prefrontal, and parietal cortex), and to a number of brainstem structures. Thus, altering PC activity with tES provides a way to modulate cerebellar outputs that influence a large number of sites in the cerebral cortex that underlie diverse functions.

Cerebellar cortical neuron responses to electric fields (E-fields) have been well characterized *in vitro* (e.g., Chan and Nicholson 1986). However, *in vivo* animal studies addressing questions related to the mechanism of ctES are scarce in the literature [20], which is

Author Manuscript Author Manuscript Author Manuscript Author Manuscript

problematic as significant differences exist between *in vivo* and *in vitro* conditions. Thus, our goal was to investigate the response of PCs to both tDCS and tACS under *in vivo* conditions. Our results demonstrate that PC simple spike activity is modulated and strongly entrained by AC stimulation over a large range of frequencies. Moreover, PC responses showed a dependence on the direction of the E-field, with significantly stronger modulation caused by rostrocaudally oriented fields as compared to fields applied mediolaterally. For tDCS, we also observed a sharp transient response at the onset and offset of the stimulation current. The results of this study shed light on some basic mechanisms of cerebellar neuromodulation by tES that may help design future human trials.

Methods

Animal surgery

Ten Sprague Dawley (SD) rats (300–350 g, male, Charles River) were used in this study to obtain PC recordings. All procedures were approved and performed in accordance to the guidelines of the Institutional Animal Care and Use Committee, Rutgers University, Newark, NJ. Animals were first anesthetized with 5% isoflurane in an induction chamber and maintained between 1 and 2% during the course of surgery. Then, they were moved to a stereotaxic head frame, and body temperature was measured with a rectal probe and regulated with a heating pad under the animal (ATC 1000, WPI). Blood oxygen level was monitored with a pulse oximeter attached to the hind paw and was always above 90% during recordings. The hair over the head was shaved and a midline skin incision was made to expose the skull over the cerebellum. The entire dorsal side of the cerebellum was opened with rongeurs. The dura mater was left intact and kept under warm saline (~34 °C as measured using an infrared thermometer) to prevent dehydration and cooling of the cerebellar cortex. The stereotaxic frame was placed inside a Faraday cage to eliminate electromagnetic interference in neural recordings. About 10 min before starting to record neural activity, the animal was transitioned from gas anesthesia to ketamine/xylazine mixture (80 mg/kg and 8 mg/kg, IP), since many studies on cerebellar electrophysiology have been conducted under this anesthesia regime, and additional doses of ketamine (20 mg/kg, IP) were injected as needed.

Electrical stimulation

To generate E-fields directed along specific axes, a stimulation electrode platform was built using four 125 μm thick Ag/AgCl wires that were affixed on a 4 × 4×1mm silicon (Polydimethylsiloxane; PDMS) board in a rectangular configuration (Fig. 1A). The distance between opposite contact pairs was 3.5 mm and the length of each contact was slightly shorter (~3.2 mm). Another Ag/AgCl wire was wrapped 3 times around a 1 mm diameter drill bit to make a helical electrode. After opening a 1.2 mm circular hole at the center of the substrate, the helical electrode was positioned into this hole. Opposing wire electrode pairs (shown in blue and red) were used to generate E-fields in the mediolateral (ML) or rostrocaudal (RC) directions. The helical electrode was used to create E-fields in the dorsoventral (DV) direction by pairing it with a Ag/AgCl wire inserted into the right hind limb. The electrode pairs were connected to the output of a voltage/current isolator unit (Model 2200, A-M Systems) through a commutator that facilitated switching between the

Author Manuscript Author Manuscript Author Manuscript Author Manuscript

electrode sets quickly. The PDMS substrate was placed over the cerebellum with its center positioned over vermis lobule 7 and secured with silk sutures tied to the frame. The hole in the center was filled with normal saline to ensure a stable interface with the helical electrode.

AC stimulation

Once stable spike activity in vermal lobule 7 was detected from a cell that was identified as a PC from its characteristic complex spikes, ten-second long sinusoidal currents were applied to the cerebellar cortex in the DV, ML, and RC directions by switching to respective electrode pairs sequentially. Sinusoidal stimulus frequency was varied systematically from 2 Hz to 100 Hz and the amplitude was varied from 50 μA to 600 μA in steps.

DC stimulation

A direct current was applied to the cerebellum through the RC electrode pair only for 20s. One or two intensity levels between 200 and 300 μA were tested. The current was injected in both directions through the electrode pair with a settling period of about 3 min between applications that allowed the activity to return to its baseline level.

E-field measurements

Two additional male SD rats similar in size to those used in stimulation experiments were anesthetized to measure the E-fields generated in the cerebellar cortex corresponding to specific current amplitudes. Five-second long sinusoidal currents, with 100 μA peak amplitude and 100 Hz frequency, were applied to the cerebellar cortex through the DV, ML, and RC electrode pairs as in the stimulation sessions. A glass micro-pipette mounted on a micromanipulator was inserted into the cerebellar cortex at five selected positions within the central hole of the stimulation electrode (Fig. 1A, inset. red Xs). Voltage measurements were obtained at depths of 200, 250, and 300 μm from the pial surface. At every recording position and depth, sinusoidal current was applied via each one of the three sets of electrode pairs. The ML and RC E-field components were calculated by taking the difference of the voltages measured at the depth that approximately corresponds to the PC layer (250 μm) by an appropriate pair of recordings (two of the four peripheral recording positions) and dividing by their separation (0.6 mm). The central recording position was used to measure the E-field component in the DV direction by taking the difference of the voltages at 200 μm and 300 μm depths and dividing by the difference in depth (100 μm). For each electrode pair, the E-fields in three orthogonal directions were calculated. The results in all PC modulation trials were expressed as a function of E-field strength by converting the applied current amplitudes to E-fields based on these measurements. Note that the E-field is not expected to be uniform in any direction in this setup. Thus, the E-field measurements were made only to demonstrate the directionality of the induced E-field by different electrode pairs.

Single unit recording and analysis

To record PC activity, a glass micropipette (3–5 MΩ) filled with normal saline was inserted at the center of the hole of the electrode platform using a 3-axis 10 μm-resolution micromanipulator through the dura and pia maters into the apex of lobule 7. Recordings

Author Manuscript Author Manuscript Author Manuscript Author Manuscript

were band-pass filtered between 100 Hz and 10 k and amplified (Model 2200, A-M Systems, Carlsborg, WA) with a gain of 1000 or 10,000, depending on spike amplitude, and sampled at 100 kHz onto a computer via a data acquisition board (NI, PCI-6071, Austin, TX). A total of 23 PCs were recorded in 10 animals, with a maximum of three PCs in a given animal. Neural signals were monitored simultaneously on an oscilloscope and audio speaker.

PCs were identified by their characteristic complex spikes, which were typically followed by a 10–30 ms pause in SS activity (Fig. 2). Recordings were all obtained at depths of ≤250 μm to ensure that they were located at the apex of the lobule, so that we would know the orientation of their dendritic tree with respect to the stimulation electrodes. For each stimulus setting, baseline PC activity was recorded before and after the stimulus period. For AC stimuli, the pre- and post-stimulation periods were each 5s, with an intervening 10-s stimulus. For the DC stimuli pre- and post-stimulation periods were 5s and 10s, respectively, and the stimulus was 20s in duration.

Spikes were detected offline in Matlab (Mathworks) with a threshold-based spike detection algorithm. For high frequency AC stimulation, recorded signals were pre-filtered with a sharp high-pass at 200 Hz, in addition to the 2nd order filters in the amplifier, to suppress the stimulation artifacts.

Results

E-field measurements

The cerebellar cortex is highly anisotropic, with many neuronal elements oriented along specific and often perpendicular axes. Because of this, the direction of the E-field may be a particularly important parameter for cerebellar stimulation, as different classes of neuronal elements may be activated by fields in different directions. Before examining this issue in detail, we first tested the ability of the stimulus electrodes to generate E-fields directed along the RC, ML and DV axes. The results show that each stimulus electrode pair produced an E-field whose amplitude was largest in the intended direction (i.e., along the axis connecting the two electrodes) but that smaller amplitude fields were present in the other two orthogonal directions. A 100 μA current applied between the specific RC, ML, and DV electrode pairs produced 1.5, 1.5, and 7.5 mV/mm fields in the direction of the electrode pair through which the current was applied. For each electrode pair, the fields produced in the other two orthogonal directions were <30% of these maximal fields, confirming that directional E-fields were generated in each case.

Spontaneous simple spike activity

To have a baseline for comparing the evoked activity, spontaneous PC simple spike activity was characterized. PCs had a mean firing rate of 40 ± 20 Hz (mean ± std) (n = 23) before any stimulation was applied. We also compared the firing rates before and after stimulation for each intensity level separately. Paired t-tests failed to show any significant difference in pre- and post-stimulus firing rates at any current level ($p > 0.11$). Thus, stimulation did not cause any immediate post-stimulus changes in average firing rates.

Author Manuscript Author Manuscript Author Manuscript Author Manuscript

Spontaneous variations in simple spike instantaneous firing rates were present in all PCs (Fig. 3, pre- and post-stim periods). To quantify this modulation, the coefficient of variation (CV) was defined as the standard deviation of the inter-spike intervals (ISI) divided by the mean ISI for the period in question. CV values of the spontaneous variations were calculated for each cell using the 5 s pre-stimulation periods (0.82 ± 0.45, mean ± std). These spontaneous variations could be obscured by stimulus-evoked activity but reemerged after the stimulus was terminated at pre-stimulus levels (post-stimulus CV = 0.79 ± 0.37, $p = 0.3$).

In order to determine if the spontaneous activity changed over the course of the experiment, spontaneous CV values during the 5 s periods before the onset of stimulations in each E-field direction were calculated. These spontaneous CVs did not differ significantly, indicating that the spontaneous variations in the firing rate did not differentially influence the calculation of the CV values in different directions. This result further confirms the absence of after-effects of the simulation on the spontaneous modulation and average firing rate.

AC stimulation

SS modulation varies with E-field direction and intensity—Fig. 4A shows how the response of a typical cell to 2 Hz AC stimulation varied with stimulus amplitude for a field directed in the RC direction. In this case, the firing rate increased during the positive phase and decreased during the negative phase, being completely suppressed at higher intensities. The maximum SS firing rates occurred slightly before the positive peak of each cycle. In general, the exact phase relationship between the stimulus current and PC firing rate changes varied between cells. In fact, increasing or decreasing spiking could be associated with either the anodic or the cathodic phases of the stimulus, and peak firing rates did not necessarily coincide with stimulus peaks. For instance, with DV current injection, which approximates the transcranial monopolar electrode montage, we observed that the firing rate increased during anodic phases and decreased during cathodic cycles in 10 out of 17 PCs, and the phase relation was reversed in the other 6 PCs.

The amplitude of SS modulation induced by the AC stimulation was quantified by calculating CVs for the stimulus period. For the cell in Fig. 4, the CV was highly correlated with stimulus intensity (Fig. 4B; r = 0.99, $p = 0.0012$, test of whether $r \neq 0$). CVs were similarly calculated and plotted as a function of intensity for all PCs (n = 17 out of 23) that were tested in all three directions (Fig. 5A), and the slopes of the individual cell regression lines were compared (Fig. 5C). From these plots, it is clear that RC- and DV-directed currents were the most consistent in producing a positive relationship between modulation depth and E-field strength, with 17 and 15 cells, respectively, showing positively sloped regression lines for RC- and DV-directed fields. Moreover, RC stimulation produced steeper slopes than DV ($p < 3 \times 10^{-3}$) or ML ($p < 3 \times 10^{-6}$) directed stimulation. ML-directed currents produced generally weaker relationships, with about half of the cells showing negatively sloped regression lines, that were not significantly different from zero, on average, one sample t-test ($p > 0.72$).

The greater slopes for the RC-directed field suggest that fields in the RC direction will have the strongest modulatory effect on PC activity. However, the spontaneous variations in SS

Author Manuscript Author Manuscript Author Manuscript Author Manuscript

activity also contribute to the overall modulation, and this contribution may be particularly significant at low AC intensities and in the ML direction where the modulation is the weakest. Thus, CV values, rather than slopes, were compared between all directions measured at a single E-field strength (7.5 mV/mm) (Fig. 5B). Consistent with the slope analysis, RC modulation was again significantly stronger than the other two directions (RC > ML, $p = 0.013$; RC > DV, two-sided, paired t-test, $p = 0.027$). However, DV was not significantly different than ML (two-sided, paired t-test, $p = 0.24$). In order to check if ML stimulation caused modulation above the noise level, we compared the CVs at this E-field intensity with the pre-stimulus period and found no significant difference ($p = 0.056$).

Spontaneous changes in firing rate are a source of noise that lowers the correlation (R^2) of the fitted lines. However, electrical stimulation for both DV and RC directions decreases the spontaneous variations and forces PCs to fire more regularly, as suggested by the high R^2 values of the regression lines. The RC and DV directions generated higher R^2 values (0.69 ± 0.32 (mean ± std) and 0.74 ± 0.31 respectively) compared to ML (0.43 ± 0.34), which agrees with the example in Fig. 4 showing significant entrainment of the SS activity during RC stimulation.

Entrainment to AC cycle—Fig. 6 summarizes the behavior of a PC under varying AC frequencies. Spontaneous simple spikes fire with ISIs varying over a wide range when there is no stimulation (top trace). Once the stimulation is initiated, the spike timings begin to synchronize with the AC stimulus phase. At low frequencies, multiple spikes occur during the positive phase and the PC completely ceases firing in the negative cycle in this example. As the stimulus frequency is increased, the number of spikes that occurs during each positive phase decreases and the spikes are limited to an increasingly smaller portion of the stimulation cycle (phase locking). When the AC frequency is raised up to 40 Hz, the cell fires only one spike per cycle that is perfectly phase-locked to the stimulus. Increasing the frequency to 100 Hz results in an increase in the overall firing frequency of the PC and the phase-locking pattern remains; however, the cell starts skipping some cycles of the AC stimulation. The bar plots on the right show the timing of the PC spikes with respect to the AC cycle. Phase locking becomes stronger with increasing frequencies as is shown by the bar plots.

During the baseline activity, the PC spike trains were characterized by positively skewed ISI distributions with a peak of 28 ms ± 33 ms (mean ± std) (n = 174) on average (Fig. 7 top panel). AC stimulation produced dramatic frequency-dependent changes in the ISI distribution. With stimulus frequencies lower than the spontaneous firing rate, a peak appeared at the lower end of the ISI plot around 5 ms (Figs. 7 and 10 Hz), reflecting the high frequency bursts that occurred within each cycle. A smaller secondary peak occurred at ISIs roughly corresponding to the interburst period at the same time (80–90 ms). As the stimulus frequency was further increased, additional peaks reflecting the subharmonics of the stimulus frequency appeared because the cell failed to fire on some of the AC cycles (e.g. the small peak at 50 ms for 40 Hz). For progressively higher frequencies, the peak corresponding to ISIs from within each burst reduced in size and the main peak corresponding to the stimulus period increased (for 20–100 Hz panels), and because the burst length decreases with frequency, the main peak increasingly became narrower around

Author Manuscript Author Manuscript Author Manuscript Author Manuscript

the stimulus period. This effect of burst length is most evident for 40 Hz stimulation in the skewed values of ISIs below 25 ms extending down to 18 ms, which is because the ISI between the last spike in a cycle and the first spike in the next cycle are less than the length of one cycle.

To assess the changes in ISI distribution between stimulus frequencies, ISIs were grouped into three categories: *intra-cycle, inter-cycle,* and *cycle-skipping* ISIs (Fig. 8). The *intra-cycle* group contains ISI values where successive spikes occur within the same AC stimulation cycle. The ISI between the last spike in a cycle and the first spike in the next was labeled as an *inter-cycle* ISI. Finally, when an ISI was greater than one cycle, indicating that at least one cycle was skipped, it was classified as *cycle-skipping*. For each PC, the number of ISIs for each category was normalized by dividing it by the total number of ISIs for that PC; thus, the sum of percentages across the three plots for the same PC at a specific frequency is equal to 100% in Fig. 8. At low frequencies, a large percentage of spikes were classified as *intra-cycle*. As the stimulus frequency is increased, the percentage of *intra-cycle* spikes decreased and those of the other two groups increased with rises in *inter-cycle* spikes rising first. Thus, a point is reached between 20 Hz and 50 Hz at which *inter-cycle* spikes form the majority and then, for most cells, decline, as *cycle-skipping* ISIs come to dominate. In a cell where the entrainment is perfect, i.e. only one spike per AC cycle and no skipped cycles, the *intra-cycle* and *cycle-skipping* groups would be zero percent, and the *inter-cycle* group would be 100%. Although none of the cells presented this pattern, most were able to track the stimulation frequency up to ~40 Hz, i.e. 0% *cycle-skipping* ISIs. However, when stimulus frequency was increased above 50 Hz, these cells started missing cycles, and by 100 Hz, only three cells could produce spikes in at least 80% of the AC cycles (Fig. 8B). Nevertheless, that all cells had a majority of inter-cycle ISIs for a stimulus frequency between 20 and 100 Hz shows that AC stimulation can strongly entrain PC spiking.

Finally, as the maximum of the inter-cycle ISI curve for the PCs varied over a wide range of frequencies, we tested whether the maximum entrainment frequency of a cell (defined as the peak of the cell's inter-cycle ISI curve) was determined by its spontaneous firing rate. However, no significant correlation was found ($r = 0.003$).

DC stimulation—DC current injections were made using the RC electrode pair because of the stronger modulation observed in this direction with AC stimulation. The stimulus intensity was selected within 3–4.5 mV/mm range based upon the level of modulation. Recordings were divided into three time intervals: pre-, post-, and during-stimulation periods. For each time interval, the mean firing rate was calculated within a 100 ms sliding window with 50 ms overlap. Anodic and cathodic stimulation (named with respect to the rostral electrode) modulated the spike rate in opposite directions (up or down) in each cell (Fig. 9), but the polarity of stimulation (anodic or cathodic) that was excitatory varied between cells. As clearly seen in the average activity from multiple cells in Fig. 10, the up-modulation response of the cells during stimulation consisted of two phases (Fig. 10 left): an initial large transient response at the onset of the stimulus followed by a settling phase. However, the time constant for the firing frequency to return to a stable level could not be captured within the 20s window of recording. At the onset of down-modulating pulses (Fig. 10 right), there is a dramatic fall of firing rate, but recovery seems marginal because the

Author Manuscript Author Manuscript Author Manuscript Author Manuscript

minimum firing rate was clipped off at zero. Following termination of the stimulus a second, oppositely directed, transient response was observed in both panels.

Discussion

In this study we demonstrated that the effect of applied E-fields on cerebellar activity is directionally dependent under *in vivo* conditions by recording PC responses to AC stimuli applied in three orthogonal directions. In particular, fields oriented in the RC and DV directions were effective in modulating PC activity, whereas those in the ML direction were not. Moreover, we demonstrated that simple spikes entrain to AC stimulation, and do so in a frequency dependent manner. Finally, we characterized the responses of PCs to both anodic and cathodic DC stimulation.

Previous reports on polarity of cerebellar modulation

Early *in vivo* studies on the cerebral cortex showed that the modulation of neuronal activity was dependent on the direction of the E-field [21–23]. Subsequently, *in vitro* studies confirmed and extended this relationship to other brain regions, including the hippocampus and cerebellum (e.g. [24,25]). Moreover, computational studies have further shown how electrode placement [26] and anatomical variations [27] affect the field distribution. In general, these studies conclude that fields generated by currents directed from the distal dendrites toward the soma will cause somatic depolarization, which will increase the excitability and activity of the neuron, whereas fields directed perpendicular to the soma-dendritic axis will be more limited in their ability to polarize a neuron (for review [28]).

Responses of PCs to applied E-fields recorded in an *in vitro* turtle cerebellum preparation are generally consistent with these rules [20]. However, predicting the responses of PCs in the mammalian cerebellum *in vivo* may be difficult for several reasons, including: 1) The mammalian cerebellum is a highly folded structure, and so the orientation of PCs (and other cells) with respect to the E-field will vary considerably [29], 2) E-field distribution may be non-uniform at the cellular level due to inhomogeneity of tissue conductivities, and 3) Synaptic effects, including from inhibitory interneurons of the cerebellar cortex, may compete with the direct polarization effects of the E-field on the PC. Therefore, the net effect may be different among PCs, even those that are in the same lobule or zone. Accordingly, in our preliminary work, the up-modulation of PC activity was associated in some cases with positive and in other cases with negative cycles of AC stimulation [30]. In addition, our prior E-field measurements in the rat brain demonstrated substantial deviation from an expected exponential decline as a function of depth, which was difficult to explain by methodological shortcomings alone [31,32] and must be the result of inhomogeneity of the conductivities in different cortical layers. Consistent with the complexity of predicting the overall effects of E-fields on cerebellar output, studies of E-field direction on cerebellar effects on other brain areas and behavior have reached contradictory conclusions, with some showing a dependence on electrode polarity [33,34], and others not [35].

Author Manuscript Author Manuscript Author Manuscript Author Manuscript

E-field direction

During tES, cortical cells may experience the E-field in different strengths in each direction depending on their position with respect to the extra-cranial electrode. Applying a unidirectional E-field at any point inside the brain with transcranial electrodes is practically impossible. Rahman et al. showed in their computational study that with transcranial electrodes E-fields have horizontal and vertical components, with the intensity of the tangential component significantly larger than the radial component [25]. We came to similar conclusions from experimental E-field data collected in the rat brain [32], and from the E-field measurements in this study where E-field intensities in the orthogonal axes were ~30% of that in the axis formed by the two electrodes. Nevertheless, the relative directionality of the E-field was strong enough for us to identify significant changes in PC modulation with E-field direction, suggesting that E-field direction may be a parameter worth considering in behavioral/clinical studies.

SS modulation vs. E-field direction

In our study, we chose the cerebellar vermis for testing, where parallel fibers run mediolaterally and intersect with the PC dendrites that ramify in the parasagittal plane. The basket and stellate cell dendritic trees lie in the parasagittal plane. Thus, the E-fields we applied in the RC, DV, and ML directions should have differentially affected these various elements, and these differences likely are the primary cause of the directional dependence we observed.

E-fields in the ML direction had the weakest effects, with barely detectable levels of modulation in most cells. The polarization of PCs is expected to be lowest in this direction due to parasagittal orientation of their dendritic trees. Therefore, the main modulatory effect on PC activity may result from the E-field effect on the parallel fibers (PFs), which lie parallel to the E-field. In fact, E-field parallel to an axon can effectively perturb the transmembrane potential along the axon as well as at its pre-synaptic terminals, and thereby influence synaptic efficacy directly. PFs synapse on and excite both PC and molecular layer interneurons (basket and stellate cells), which inhibit PCs. Thus, direct modulatory effects of PFs on PCs may be balanced by that of the indirect effects through interneurons, resulting in a relatively small net effect on PC activity.

Ketamine-xylazine anesthesia has been reported to reduce activity in the cerebellar cortex compared to the awake state [36,37], (however, we note that the simple spike rates found in the present and other studies using ketamine anesthesia are well within the ranges of rates reported for awake animals), and it may have altered the direct and indirect modulatory effects of the E-field on the PCs in this study. Despite anesthesia, however, there still would have been some modulation with ML E-fields, if the indirect parallel fiber mediated effects were substantial.

RC E-fields generated significantly stronger modulation than the ML stimulation, and indeed, produced the strongest modulation of the three directions that were tested. The RC E-field is expected to polarize most strongly the large dendritic tree of PCs since the E-fields of bipolar electrodes decrease quickly with depth and thus should be relatively smaller at the

Author Manuscript Author Manuscript Author Manuscript Author Manuscript

level of the PC soma. We tried to record from the PCs at similar depths near the surface and in the center of the apex of the lobule to ensure that the E-field intensity was approximately the same for all recorded cells. Hyperpolarization of the dendrites is expected to increase the amplitude of EPSPs [38] and should also decrease that of IPSPs, both of which should increase PC activity while the depolarization of dendrites is expected to cause the opposite effect. In contrast, DV stimulation is a monopolar configuration and its E-field should reach down to the PC somas more effectively than the RC and ML E-fields. Thus, the larger modulatory effect of the RC stimulation suggests that modulation of synaptic efficacy on the dendrites had a stronger effect than polarization of the soma under our condition. In addition, a DV E-field would likely excite the deep lying Golgi cells, and that could also limit the PC responses.

With respect to direct E-field effects on the soma, the Chan et al. study showed that both stellate cells and PCs are modulated by AC stimulation when the E-field is oriented along the somatodendritic axis [39]. On the other hand, computer models based on passive cell properties predict that cellular polarization is directly correlated with the distance between the soma and the apical dendrites. Radman et al. showed in a slice preparation that the larger the cortical cells are, the more they are polarized by the extracellular E-field [40] as predicted by volume conductor theory. Among the neurons in the cerebellar cortex, the PCs have the largest soma (~30 μm) and soma-dendrite length, and an extensive dendritic tree. Therefore, the direct effect of the E-field on the PCs should be larger compared to the indirect modulation via inhibitory cells.

With DV AC field injection (normal to the cortex), we observed that, in most PCs, the firing rate increased during anodic phases and decreased during cathodic cycles, in agreement with previous studies [22,24,39,41]. However, 6 of the PCs responded to stimulation in the reversed manner, i.e. activity increased during the negative cycle and *vice versa*. Dendritic morphology and orientation relative to the E-field play a significant role in determining the cellular modulation [42,43]. Even though the dendritic trees of PCs spread parasagittally in the vermis, their orientation within the parasagittal plane and their specific morphology can vary substantially, and this may have been responsible for the reversed response in 6 PCs and the lack of modulation in 1 PC that we recorded from.

Entrainment of SSs by AC

Rhythmic activity spanning a large range of frequencies has been reported for the cerebellum. For example, PC complex spikes show transient ~10 Hz as well as slower (~1 Hz) rhythmicity induced via climbing fiber activity from the inferior olive [44,45]. In contrast, simple spikes and local fields can show oscillatory activity over much higher frequencies, ones that can be as high as 160–240Hz [46], and they can show a phase-amplitude relation to the oscillations in the cerebrum [46,47] that suggests exchange of information. It is conceivable that the local field potential oscillations commonly observed in the cerebellum may be entrained with tACS, as demonstrated in other parts of the brain [48–51], leading to strengthening of cerebello-cerebral circuits, which could potentially facilitate motor and cognitive functions, as suggested by several human studies [52–54]. Naro et al. applied AC stimulation at various frequencies to the cerebellum in healthy individuals and

Author Manuscript Author Manuscript Author Manuscript Author Manuscript

recorded muscle potentials evoked by stimulation of the contralateral primary motor cortex [55]. They noted that 50 Hz stimulation led to reduction in the cerebello-brain inhibition (CBI) effect and facilitation of the muscle evoked potentials (MEPs). However, 10 Hz and 300 Hz stimulation resulted in mild or no effect on the CBI and MEPs. Miyaguchi et al. also applied AC at gamma (70 Hz) frequencies to the motor and cerebellar cortices and reported that simultaneous stimulation of these two regions improved the visuomotor performance [56]. In another study, the same group provided further evidence that the reason for this increase was the enhancement of cerebello-cerebral connections [57].

The present results show that entrainment of PC simple spike activity with exogenous E-fields is feasible. Some PCs followed AC stimulation cycle-by-cycle up to 100 Hz, while others were not able to track the stimulus frequency and began skipping cycles before reaching 100 Hz, which could be related to the spontaneous firing rates. There are alternating bands of zebrin+ and zebrin-across the cerebellar cortex defined by the expression of aldolase C enzyme. PCs in zebrin-zones are known to fire at about twice higher rates than those in zebrin + bands. The PCs with high SS rates may be following the stimulus frequency up to higher rates. Indeed, the spontaneous firing rates distributed in a large range in our data and resembled bimodal distribution (not shown). However, there was no correlation between the maximum entrainment frequency and the spontaneous rates. Thus, we have to assume that other electrophysiological factors including the specific cerebello-cerebral connection and the functional network that the PC is a part of might have played a role in maximum entrainment frequency.

Electrode placement

The electrodes were placed epidurally, instead of attaching them on the skin as in human trials, to maximize reproducibility of the E-field strengths by eliminating the extra layers of tissue and skull.

Asamoah et al. raised a concern that some of the observed results could result from indirect effects of stimulus current [58]. Placing the stimulation electrode on the skin can cause sensory stimulation and affect the cerebellar activity through secondary pathways. Epidural placement of the stimulating electrode eliminated this potential source of error. The strong dependence of the PC modulation on the electrode orientation, where the only difference is the direction of the stimulation electrode in different trials, proved that such secondary stimulation effects did not play a role.

DC modulation

With DC stimulation, the electrodes corrode quickly at high current densities. Our electrodes were small to achieve localization and thus the current density at the electrode surface was larger than that of standard transcranial electrodes. Hence, we applied the DC stimulation in the most effective direction with a single E-field value only (as determined with AC stimulation first) to ensure that the electrode characteristics were not changing during stimulation.

We observed polarity dependent modulation with DC stimulation, as expected. Unlike tDCS studies in awake subjects that use ramp-up and ramp-down periods, we applied the DC with

Author Manuscript Author Manuscript Author Manuscript Author Manuscript

rectangular shape, and this caused drastic jumps in the PC firing rates at the onset and offset of the stimulation. The sharp change in SS firing rates indicates that the PCs have a response to fast-changing or high frequency components of the stimulus current, which is in line with the results of high frequency AC stimulation. After the initial jump, spike activity tends to return to the baseline levels with a time-constant that is on the order of 10–20s. Thus, the single cell data reaffirms the importance of turning the current on slowly in clinical tDCS [59] in order to prevent a transient overshoot in PC activity, even if sensory stimulation under the skin electrodes is not an issue. It should also be mentioned that the strength of the PC response to the DC field may vary depending upon the E-field direction, as it was observed with AC stimulation.

E-field intensity

With finite element models and measurements in human cadavers, the E-fields that are effective were shown to be around 1 mV/mm [60–62]. In this study, we employed fields that were similar in strength, and in accordance to these reports we observed a significant modulatory effect at 0.75–1.5 mV/mm when the E-field was applied in RC and DV directions. This suggests that the results of this study will be applicable to human studies. However, in order to increase signal-to-noise ratio in the data, we also used higher E-field intensities to quantify more robustly the relation between the E-field strength and the induced modulatory effect.

Acknowledgments

This work was supported by the National Institutes of Health [R21 NS101386].

References

[1]. Johnson MD, Lim HH, Netoff TI, Connolly AT, Johnson N, Roy A, et al. Neuromodulation for brain disorders: challenges and opportunities. IEEE Trans Biomed Eng 2013;60(3):610–24. [PubMed: 23380851]

[2]. Bikson M, Grossman P, Thomas C, Zannou AL, Jiang J, Adnan T, et al. Safety of transcranial direct current stimulation: evidence based update 2016. Brain Stimul 2016;9(5):641–61. [PubMed: 27372845]

[3]. Antal A, Alekseichuk I, Bikson M, Brockmoller J, Brunoni AR, Chen R, et al. Low intensity transcranial electric stimulation: safety, ethical, legal regulatory and application guidelines. Clin Neurophysiol 2017;128(9):1774–809. [PubMed: 28709880]

[4]. Hashemirad F, Zoghi M, Fitzgerald PB, Jaberzadeh S. The effect of anodal transcranial direct current stimulation on motor sequence learning in healthy individuals: a systematic review and meta-analysis. Brain Cognit 2016;102: 1–12. [PubMed: 26685088]

[5]. Reis J, Fritsch B. Modulation of motor performance and motor learning by transcranial direct current stimulation. Curr Opin Neurol 2011;24(6):590–6. [PubMed: 21968548]

[6]. van Dun K, Bodranghien FCAA, Mariën P, Manto MU. tDCS of the cerebellum: where do we stand in 2016? Technical issues and critical review of the literature. Front Hum Neurosci 2016;10:199. [PubMed: 27242469]

[7]. Lang N, Siebner HR, Ward NS, Lee L, Nitsche MA, Paulus W, et al. How does transcranial DC stimulation of the primary motor cortex alter regional neuronal activity in the human brain? Eur J Neurosci 2005;22(2):495–504. [PubMed: 16045502]

[8]. Conley AC, Fulham WR, Marquez JL, Parsons MW, Karayanidis F. No effect of anodal transcranial direct current stimulation over the motor cortex on response-related ERPs during a conflict task. Front Hum Neurosci 2016;10: 384. [PubMed: 27547180]

Author Manuscript Author Manuscript Author Manuscript Author Manuscript

[9]. Verhage MC, Avila EO, Frens MA, Donchin O, van der Geest JN. Cerebellar tDCS does not enhance performance in an implicit categorization learning task. Front Psychol 2017;8:476. [PubMed: 28424645]

[10]. Summers RLS, Chen M, Hatch A, Kimberley TJ. Cerebellar transcranial direct current stimulation modulates corticospinal excitability during motor training. Front Hum Neurosci 2018;12:118. [PubMed: 29686609]

[11]. Hardwick RM, Celnik PA. Cerebellar direct current stimulation enhances motor learning in older adults. Neurobiol Aging 2014;35(10):2217–21. [PubMed: 24792908]

[12]. Buckner Randy L The cerebellum and cognitive function: 25 Years of insight from anatomy and neuroimaging. Neuron 2013;80(3):807–15. [PubMed: 24183029]

[13]. Van Overwalle F, Baetens K, Mariën P, Vandekerckhove M. Social cognition and the cerebellum: a meta-analysis of over 350 fMRI studies. Neuroimage 2014;86:554–72. [PubMed: 24076206]

[14]. Block H, Celnik P. Stimulating the cerebellum affects visuomotor adaptation but not intermanual transfer of learning. Cerebellum 2013;12(6):781–93. [PubMed: 23625383]

[15]. Pope PA, Miall RC. Task-specific facilitation of cognition by cathodal transcranial direct current stimulation of the cerebellum. Brain stimulation 2012;5(2):84–94. [PubMed: 22494832]

[16]. Blenkinsop TA, Lang EJ. Synaptic action of the olivocerebellar system on cerebellar nuclear spike activity. J Neurosci 2011;31(41):14708–20. [PubMed: 21994387]

[17]. Tang T, Blenkinsop TA, Lang EJ. Complex spike synchrony dependent modulation of rat deep cerebellar nuclear activity. eLife 2019;8:e40101. [PubMed: 30624204]

[18]. Person AL, Raman IM. Purkinje neuron synchrony elicits time-locked spiking in the cerebellar nuclei. Nature 2011;481(7382):502–5. [PubMed: 22198670]

[19]. De Schutter E, Steuber V. Patterns and pauses in Purkinje cell simple spike trains: experiments, modeling and theory. Neuroscience 2009;162(3): 816–26. [PubMed: 19249335]

[20]. Gardner-Medwin AR, Nicholson C. Changes of extracellular potassium activity induced by electric current through brain tissue in the rat. J Physiol 1983;335: 375–92. [PubMed: 6875884]

[21]. Purpura DP, McMurtry JG. Intracellular activities and evoked potential changes during polarization OF motor cortex. J Neurophysiol 1965;28(1): 166–85. [PubMed: 14244793]

[22]. Bindman LJ, Lippold OC, Redfearn JW. The action OF brief polarizing currents ON the cerebral cortex OF the rat (1) during current flow and (2) IN the production OF long-lasting after-effects. J Physiol 1964;172(3):369–82. [PubMed: 14199369]

[23]. Creutzfeldt OD, Fromm GH, Kapp H. Influence of transcortical d-c currents on cortical neuronal activity. Exp Neurol 1962;5(6):436–52. [PubMed: 13882165]

[24]. Bikson M, Inoue M, Akiyama H, Deans JK, Fox JE, Miyakawa H, et al. Effects of uniform extracellular DC electric fields on excitability in rat hippocampal slices in vitro. J Physiol 2004;557(1):175–90. [PubMed: 14978199]

[25]. Rahman A, Reato D, Arlotti M, Gasca F, Datta A, Parra LC, et al. Cellular effects of acute direct current stimulation: somatic and synaptic terminal effects. J Physiol 2013;591(10):2563–78. [PubMed: 23478132]

[26]. Bikson M, Datta A, Rahman A, Scaturro J. Electrode montages for tDCS and weak transcranial electrical stimulation: role of “return” electrode’s position and size. Clin Neurophysiol 2010;121(12):1976–8. [PubMed: 21035740]

[27]. Parazzini M, Rossi E, Ferrucci R, Liorni I, Priori A, Ravazzani P. Modelling the electric field and the current density generated by cerebellar transcranial DC stimulation in humans. Clin Neurophysiol 2014;125(3):577–84. [PubMed: 24176297]

[28]. Ranck JB. Which elements are excited in electrical stimulation of mammalian central nervous system: a review. Brain Res 1975;98(3):417–40. [PubMed: 1102064]

[29]. Rahman A, Toshev PK, Bikson M. Polarizing cerebellar neurons with transcranial direct current stimulation. Clin Neurophysiol 2014;125(3):435–8. [PubMed: 24176296]

[30]. Modulation of multiunit spike activity by transcranial AC stimulation (tACS) in the rat cerebellar cortex. In: Asan AS, Sahin M, editors. 2019 41st annual international conference of the IEEE engineering in medicine and biology society. EMBC); 2019 23–27 July 2019.

Author Manuscript Author Manuscript Author Manuscript Author Manuscript

[31]. Electric fields induced by transcutaneous and intracranial current injections in the rat brain. In: Asan AS, Gok S, Sahin M, editors. 2018 40th annual international conference of the IEEE engineering in medicine and biology society. EMBC); 2018 18–21 July 2018.

[32]. Asan AS, Gok S, Sahin M. Electrical fields induced inside the rat brain with skin, skull, and dural placements of the current injection electrode. PLOS ONE 2019;14(1):e0203727. [PubMed: 30629578]

[33]. Galea JM, Jayaram G, Ajagbe L, Celnik P. Modulation of cerebellar excitability by polarity-specific noninvasive direct current stimulation. J Neurosci 2009;29(28):9115–22. [PubMed: 19605648]

[34]. Jayaram G, Tang B, Pallegadda R, Vasudevan EVL, Celnik P, Bastian A. Modulating locomotor adaptation with cerebellar stimulation. J Neurophysiol 2012;107(11):2950–7. [PubMed: 22378177]

[35]. Shah B, Nguyen TT, Madhavan S. Polarity independent effects of cerebellar tDCS on short term ankle visuomotor learning. Brain Stimulation 2013;6(6): 966–8. [PubMed: 23711765]

[36]. Bengtsson F, Jörntell H. Ketamine and xylazine depress sensory-evoked parallel fiber and climbing fiber responses. J Neurophysiol 2007;98(3):1697–705. [PubMed: 17615140]

[37]. Ordek G, Groth JD, Sahin M. Differential effects of ketamine/xylazine anesthesia on the cerebral and cerebellar cortical activities in the rat. J Neurophysiol 2012;109(5):1435–43. [PubMed: 23236007]

[38]. Kabakov AY, Muller PA, Pascual-Leone A, Jensen FE, Rotenberg A. Contribution of axonal orientation to pathway-dependent modulation of excitatory transmission by direct current stimulation in isolated rat hippocampus. J Neurophysiol 2012;107(7):1881–9. [PubMed: 22219028]

[39]. Chan CY, Nicholson C. Modulation by applied electric fields of Purkinje and stellate cell activity in the isolated turtle cerebellum. J Physiol 1986;371: 89–114. [PubMed: 3701658]

[40]. Radman T, Ramos RL, Brumberg JC, Bikson M. Role of cortical cell type and morphology in subthreshold and suprathreshold uniform electric field stimulation in vitro. Brain stimulation 2009;2(4):215–28. e2283. [PubMed: 20161507]

[41]. Reato D, Rahman A, Bikson M, Parra LC. Low-intensity electrical stimulation affects network dynamics by modulating population rate and spike timing. J Neurosci 2010;30(45):15067–79. [PubMed: 21068312]

[42]. Aspart F, Remme MWH, Obermayer K. Differential polarization of cortical pyramidal neuron dendrites through weak extracellular fields. PLoS Comput Biol 2018;14(5):e1006124. [PubMed: 29727454]

[43]. Kronberg G, Bridi M, Abel T, Bikson M, Parra LC. Direct current stimulation modulates LTP and LTD: activity dependence and dendritic effects. Brain stimulation 2017;10(1):51–8. [PubMed: 28104085]

[44]. Lang EJ. Organization of olivocerebellar activity in the absence of excitatory glutamatergic input. J Neurosci 2001;21(5):1663. [PubMed: 11222657]

[45]. Lang EJ, Sugihara I, Welsh JP, Llinas R. Patterns of spontaneous Purkinje cell complex spike activity in the awake rat. J Neurosci 1999;19(7):2728. [PubMed: 10087085]

[46]. De Zeeuw CI, Hoebeek FE, Schonewille M. Causes and consequences of oscillations in the cerebellar cortex. Neuron 2008;58(5):655–8. [PubMed: 18549777]

[47]. Courtemanche R, Robinson JC, Aponte DI. Linking oscillations in cerebellar circuits. Front Neural Circ 2013;7:125.

[48]. Helfrich Randolph F, Schneider Till R, Rach S, Trautmann-Lengsfeld Sina A, Engel Andreas K, Herrmann Christoph S. Entrainment of brain oscillations by transcranial alternating current stimulation. Curr Biol 2014;24(3):333–9. [PubMed: 24461998]

[49]. Polanía R, Nitsche Michael A, Korman C, Batsikadze G, Paulus W. The importance of timing in segregated theta phase-coupling for cognitive performance. Curr Biol 2012;22(14):1314–8. [PubMed: 22683259]

[50]. Fröhlich F, McCormick DA. Endogenous electric fields may guide neocortical network activity. Neuron 2010;67(1):129–43. [PubMed: 20624597]

Author Manuscript Author Manuscript Author Manuscript Author Manuscript

[51]. Zaehle T, Rach S, Herrmann CS. Transcranial alternating current stimulation enhances individual alpha activity in human EEG. PLOS ONE 2010;5(11): e13766. [PubMed: 21072168]

[52]. Alalade E, Denny K, Potter G, Steffens D, Wang L. Altered cerebellar-cerebral functional connectivity in geriatric depression. PLOS ONE 2011;6(5):e20035. [PubMed: 21637831]

[53]. Pope P, Miall R. Restoring cognitive functions using non-invasive brain stimulation techniques in patients with cerebellar disorders. Front Psychiatr 2014;5(33).

[54]. Watson T, Becker N, Apps R, Jones M. Back to front: cerebellar connections and interactions with the prefrontal cortex. Front Syst Neurosci 2014;8(4).

[55]. Naro A, Leo A, Russo M, Cannavo A, Milardi D, Bramanti P, et al. Does transcranial alternating current stimulation induce cerebellum plasticity? Feasibility, safety and efficacy of a novel electrophysiological approach. Brain Stimulation 2016;9(3):388–95. [PubMed: 26946958]

[56]. Miyaguchi S, Otsuru N, Kojima S, Saito K, Inukai Y, Masaki M, et al. Transcranial alternating current stimulation with gamma oscillations over the primary motor cortex and cerebellar hemisphere improved visuomotor performance. Front Behav Neurosci 2018;12:132. [PubMed: 30034329]

[57]. Miyaguchi S, Otsuru N, Kojima S, Yokota H, Saito K, Inukai Y, et al. Gamma tACS over M1 and cerebellar hemisphere improves motor performance in a phase-specific manner. Neurosci Lett 2019;694:64–8. [PubMed: 30445151]

[58]. Asamoah B, Khatoun A, Mc Laughlin M. tACS motor system effects can be caused by transcutaneous stimulation of peripheral nerves. Nat Commun 2019;10(1):266. [PubMed: 30655523]

[59]. Bikson M, Grossman P, Thomas C, Zannou AL, Jiang J, Adnan T, et al. Safety of transcranial direct current stimulation: evidence based update 2016. Brain stimulation 2016;9(5):641–61. [PubMed: 27372845]

[60]. Vöröslakos M, Takeuchi Y, Brinyiczki K, Zombori T, Oliva A, Fernández-Ruiz A, et al. Direct effects of transcranial electric stimulation on brain circuits in rats and humans. Nat Commun 2018;9(1):483. [PubMed: 29396478]

[61]. Huang Y, Liu AA, Lafon B, Friedman D, Dayan M, Wang X, et al. Measurements and models of electric fields in the in vivo human brain during transcranial electric stimulation. eLife 2017;6:e18834. [PubMed: 28169833]

[62]. Thair H, Holloway AL, Newport R, Smith AD. Transcranial direct current stimulation (tDCS): a beginner's guide for design and implementation. Front Neurosci 2017;11:641. [PubMed: 29213226]

[63]. Created.with.Biorender.com; 2020.

Author Manuscript Author Manuscript Author Manuscript Author Manuscript

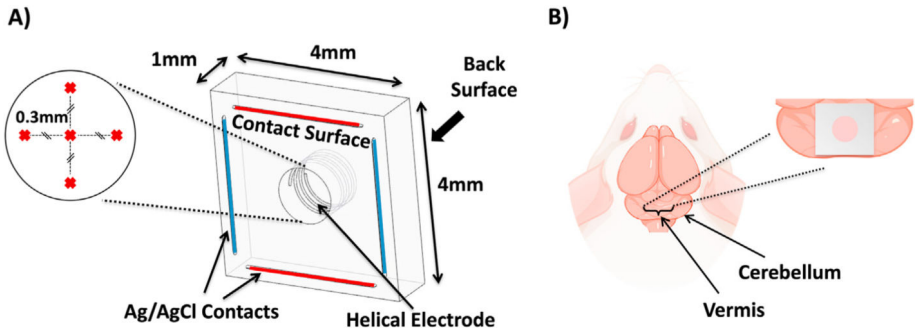

Fig. 1.

A) Computer drawing of stimulation electrode. Four Ag/AgCl wires were affixed on the PDMS substrate as shown and used to apply E-field from ML (red pair) and RC (blue pair) directions. Another Ag/AgCl helical electrode was placed in the central hole to apply stimulation in the DV direction. The circle on the left end represents the hole opened at the center of PDMS stimulating electrode and red X's show points for E-field measurements. **B)** Schematic showing the placement of the stimulation electrode on the cerebellar cortex with its center on lobule 7 of the vermis [63]. (For interpretation of the references to color in this figure legend, the reader is referred to the Web version of this article.)

Author Manuscript Author Manuscript Author Manuscript Author Manuscript

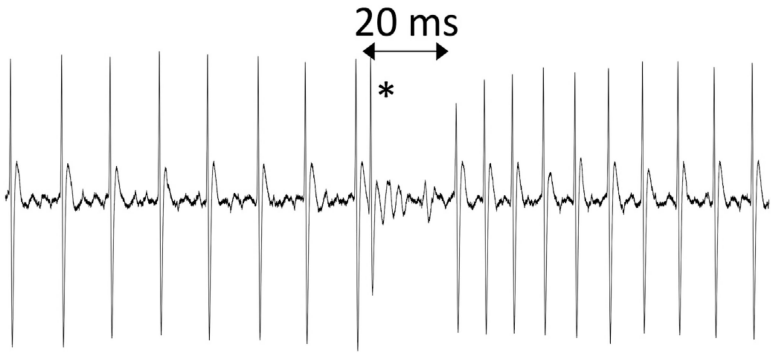

Fig. 2.

An example of a PC recording demonstrating a short pause in the simple spikes following a complex spike (star).

Author Manuscript Author Manuscript Author Manuscript Author Manuscript

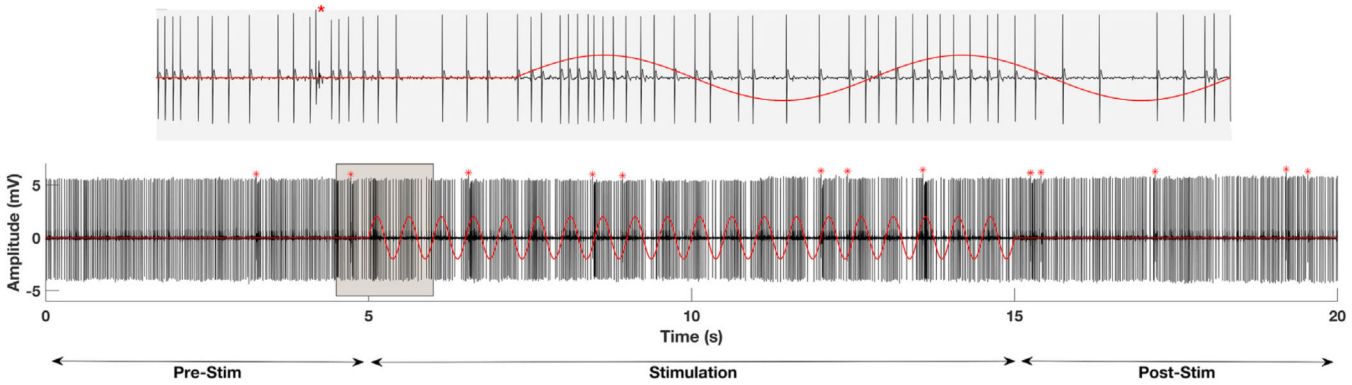

Fig. 3.

An episode of PC activity during RC AC stimulation with 3mv/mm amplitude. The red sinusoidal trace represents the injected current at 2 Hz. The upper row shows a short segment of the recorded signal on an expanded time scale where the spike frequency increases during positive cycles of the stimulus current and *vice versa*. Complex spikes are marked with red asterisks. (For interpretation of the references to color in this figure legend, the reader is referred to the Web version of this article.)

Author Manuscript Author Manuscript Author Manuscript Author Manuscript

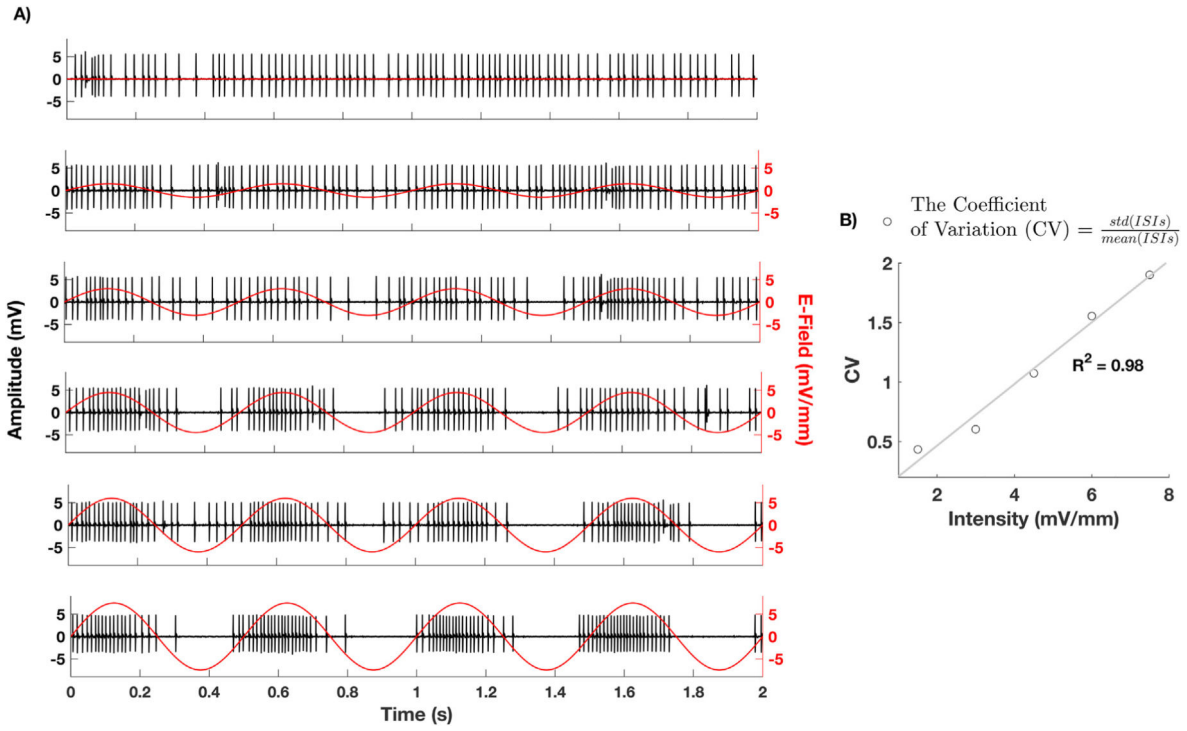

Fig. 4.

A) A typical PC response at varying amplitudes of 2 Hz sinusoidal E-field applied rostrocaudally in an ascending order, indicated by the red traces. The first row contains the baseline PC activity. The spike frequency increases during positive phases and decreases during negative phases of the stimulus current, although some phase shift may also be present. The level of spike-frequency modulation is correlated positively with the applied E-field intensity in this example. **B)** CV vs. stimulation current intensity for the recordings shown on the left. (For interpretation of the references to color in this figure legend, the reader is referred to the Web version of this article.)

Author Manuscript Author Manuscript Author Manuscript Author Manuscript

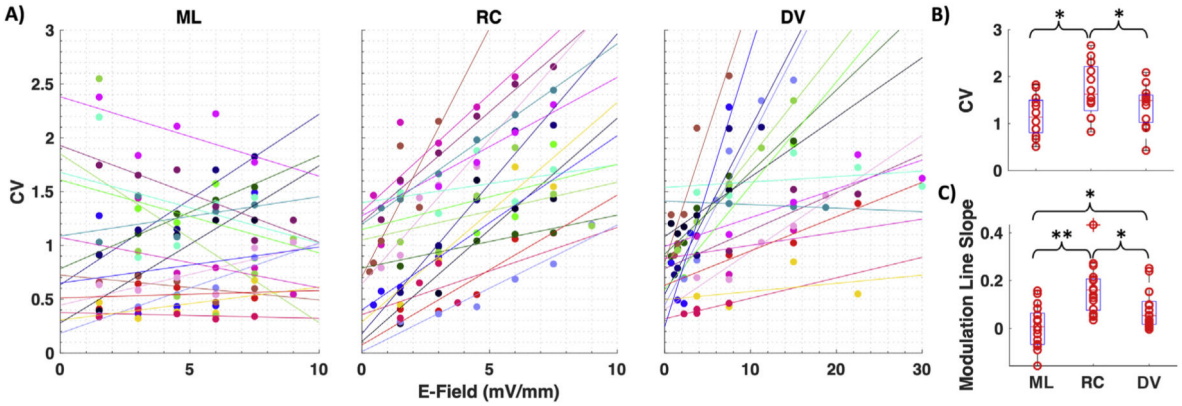

Fig. 5.

A) Incremental levels of E-fields are applied to the cerebellar cortex in ML, RC and DV directions respectively and modulation indices are plotted from a total of 17 PCs, coded by the same color in all three plots. Each dot represents a single episode of recording at a specific E-field strength from the PC. Linear lines were fitted to the CV values at different E-fields separately. **B)** Box whisker plots for comparison of modulation effectiveness for E-fields in different directions. Direct comparison of modulation indices between different E-field directions at a single intensity of 7.5 mV/mm. RC direction generates significantly stronger modulation level than both ML and DV directions (two-sided paired *t*-test, p = 0.013, p = 0.027). **C)** Each circle represents a slope of a specific line in Fig. 5a. Two-sided paired t-tests indicate that RC stimulation generates significantly higher modulation level compared to both ML (**$p < 3 \times 10^{-6}$) and DV (*$p < 3 \times 10^{-3}$) directions. DV also generates significantly higher modulation than ML direction (*p < 0.015). (+): outliers. (For interpretation of the references to color in this figure legend, the reader is referred to the Web version of this article.)

Author Manuscript Author Manuscript Author Manuscript Author Manuscript

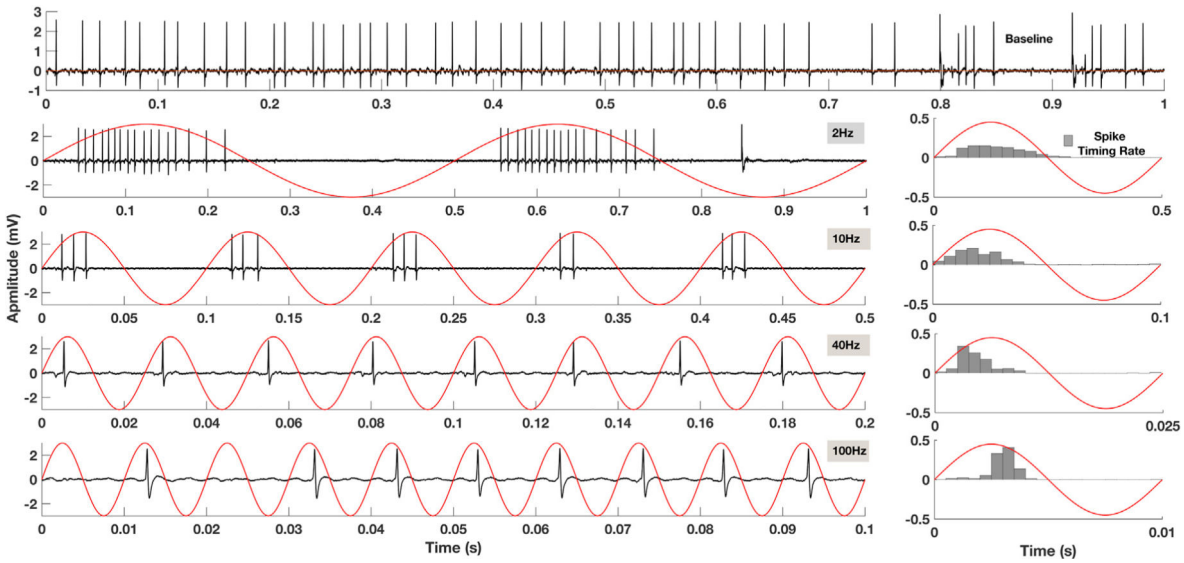

Fig. 6.

PC response to varying AC frequencies applied rostrocaudally with 4.5 mV/mm intensity. The first row shows the baseline PC activity, and rows below demonstrate the PC response to AC stimulation at 2, 10, 40 and 100 Hz respectively. The PC activity synchronizes with applied AC cycles. The activity pattern within each cycle is burst-like at low frequencies of the stimulus, whereas at higher frequencies the number of spikes that occur in an AC cycle decreases and spike timings become strongly locked to the stimulation cycle. Histogram plots on the right show the number of spikes that occur at specific time points during the stimulation cycle. The cycle was divided into 20 time bins.

Author Manuscript Author Manuscript Author Manuscript Author Manuscript

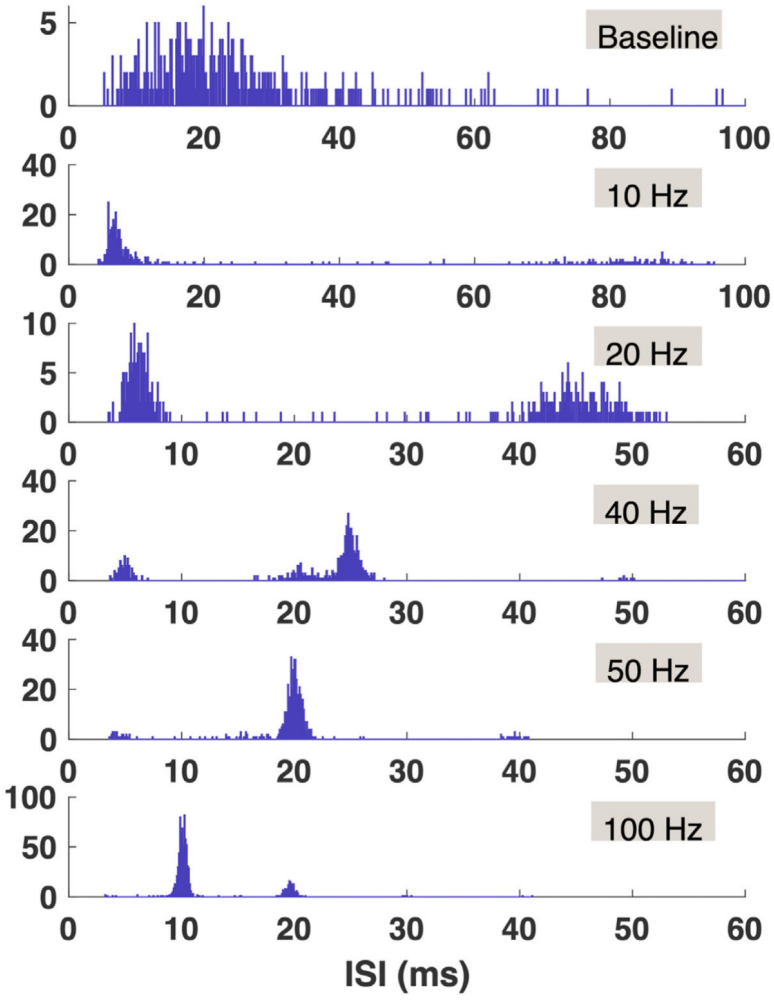

Fig. 7.

Inter-Spike-Interval (ISI) distribution at different stimulation frequencies with 4.5 mV/mm intensity. ISIs scatter in a large range during the baseline activity. Low frequency AC applications at 10 and 20 Hz cause a peak at short ISIs around 6 ms. With the increase of AC frequencies, ISIs gather around the values that corresponded to the stimulus cycle lengths, and their multiples.

Author Manuscript Author Manuscript Author Manuscript Author Manuscript

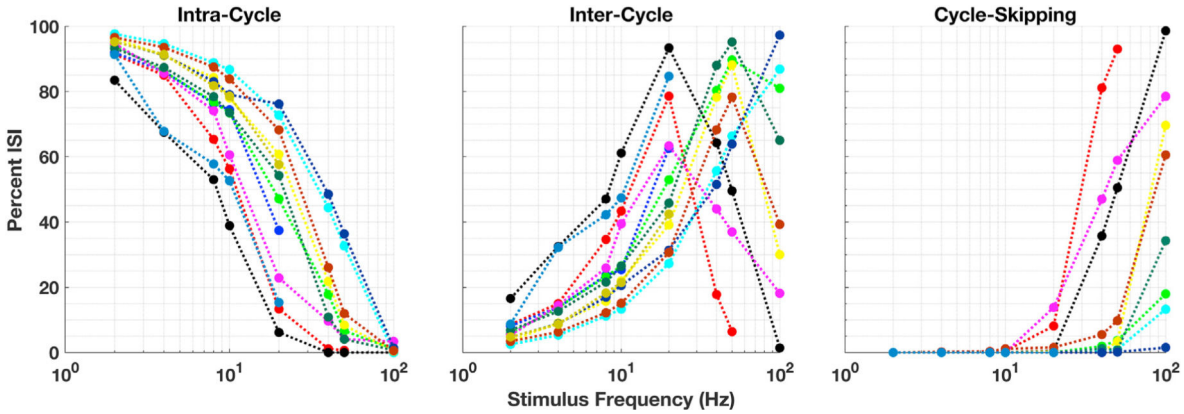

Fig. 8.

Percent of different ISI types as a function of stimulus frequency. ISIs were divided into three groups: intra-cycle, inter-cycle, and cycle-skipping. Each color represents measurements from a specific PC. Twelve different PCs were used in this analysis, and color coded. The percentage of intra-cycle spikes is high at low frequencies and decays when the AC frequency is increased, as also seen in Fig. 6. In each cell, the AC stimulus intensity was selected such that the modulation depth was clearly appreciable through the audio monitor and retrospectively found to be within 1.5–6 mV/mm range. (For interpretation of the references to color in this figure legend, the reader is referred to the Web version of this article.)

Author Manuscript Author Manuscript Author Manuscript Author Manuscript

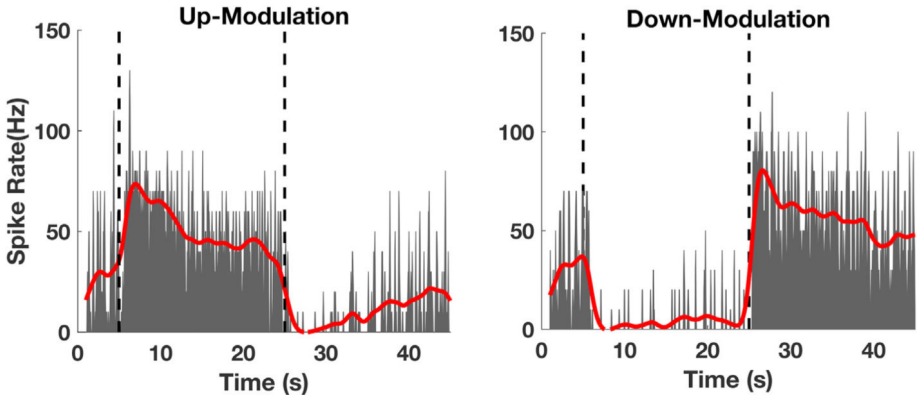

Fig. 9.

Firing pattern of a PC during DC modulation. The mean firing rate as a function of time was calculated in a 100 ms sliding window and fitted by a smoothing spline (red trace). Sharp shifts in the spike rates were observed at the onset and the offset of the DC stimulation, and the observed effect was reversed based on the polarity of the stimulus. (For interpretation of the references to color in this figure legend, the reader is referred to the Web version of this article.)

Author Manuscript Author Manuscript Author Manuscript Author Manuscript

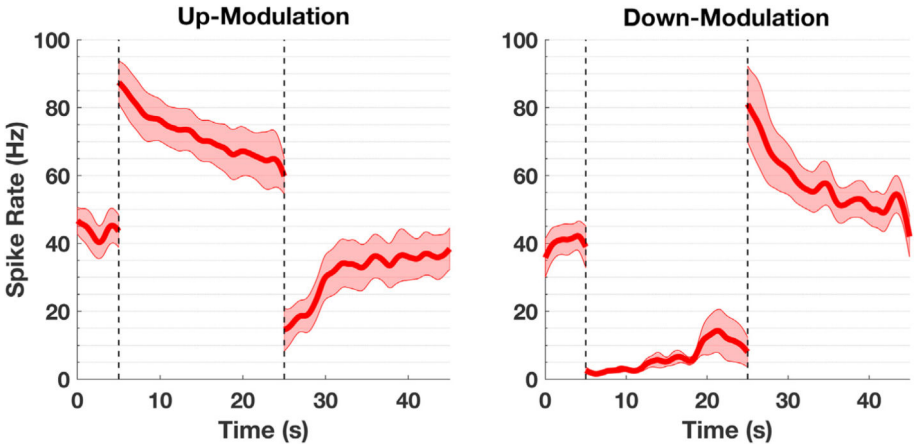

Fig. 10.

The mean spike rates from 6 different PCs during DC stimulation as a function of time. The shaded areas represent the standard error (SE). Dotted lines show the onset and offset time points of the stimulation.